DOI: 10.1002/ejoc.201101584

Design of New Tetrazine–Triphenylamine Bichromophores – Fluorescent Switching by Chemical Oxidation

Cassandre Quinton,[a] Valérie Alain-Rizzo,*[a] Cécile Dumas-Verdes,*[a] Gilles Clavier,[a] Fabien Miomandre,[a] and Pierre Audebert*[a]

Keywords: Donor–acceptor systems / Synthesis design / Redox chemistry / Fluorescence / Molecular modeling

Original new fluorescent and electroactive compounds have been prepared, which feature two different fluorescent groups linked through an oxygen atom spacer. We describe here the synthesis, photophysical and electrochemical properties and their interplay, and our theoretical calculations. These molecules are composed of two fluorophores, an electron-rich triphenylamine unit and an electron-poor tetrazine unit. Although the bichromophores are not fluorescent in the neutral state due to a photoinduced electron transfer from the triphenylamine unit to the tetrazine unit, one can restore the fluorescence by oxydation of the triphenylamine moiety. Thus, a redox-fluorescent switch has been realized.

Introduction

We are interested in the study of fluorescent electroactive chromophores based on tetrazines[1] and boron–dipyrromethene (BODIPY).[2] These molecules present different photophysical properties according to the redox state of the molecule (neutral, oxidized or reduced). For example, interplay between fluorescence and redox characteristics in the case of 3-chloro-6-methoxytetrazine could lead to a reversible switching of fluorescence (also called electrofluorochromism).[3] Although there is interest in and possible applications for the reversible fluorescent electrochemical switch of a molecule (or oligomer) composed of a single unit that is both electroactive and fluorescent,[3] multiple fluorophore systems present their own advantages.[2,4] Indeed, instead of an on–off two-state system, it should be possible to prepare dyads that display off-to-on fluorescent switching upon redox activation. Such dyads should present complementary properties to 3-chloro-6-methoxytetrazine. Hence, dyads composed of an electroactive donating group and a fluorophore accepting group should be good candidates for redox-fluorescent switchable devices.[5]

Tetrazines are particularly well adapted fluorophores for the accepting unit.[1] Triphenylamine compounds are well-known electron-rich derivatives, which are used in many applications, such as organic optoelectronics[6] and electrochromism,[7] and could be a good choice as a partner fluorophore as these molecules mostly display extremely stable cation radicals, which can be formed at moderate oxidizing potentials. Hence, tetrazine–triphenylamine dyads could behave as a two-state redox-mediated off–on fluorescent switches (Figure 1).

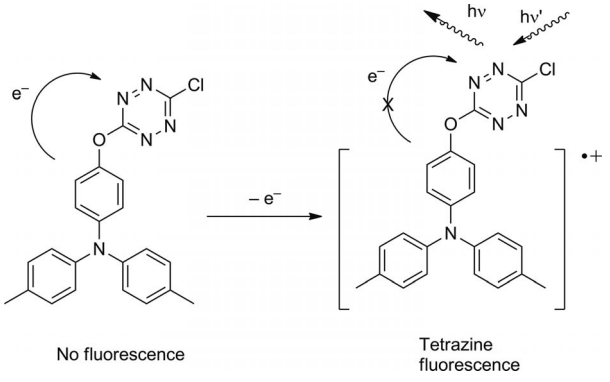

Figure 1. Two redox-state system with different fluorescent properties.

We have prepared several dyads, which should meet the above requirements and feature one or two triphenylamine moieties that bear different groups on their *para* positions,

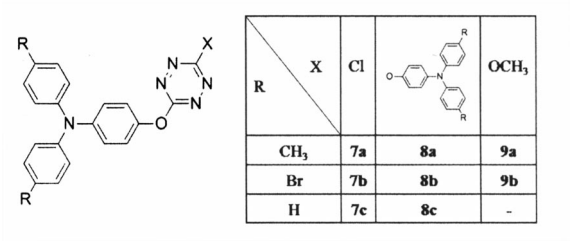

Figure 2. Design of dyads.

[a] PPSM, CNRS UMR8531, ENS Cachan, UniverSud
61 Avenue du Président Wilson, 94235 Cachan, France
Fax: +33-1-47402454
E-mail: audebert@ppsm.ens-cachan.fr

Supporting information for this article is available on the WWW under http://dx.doi.org/10.1002/ejoc.201101584.

linked by an oxygen atom to a chloro- or alkoxytetrazine, which represents the electron-poor fluorescent moiety (Figure 2).

We have investigated the photophysical and electrochemical properties and carried out theoretical quantum calculations of the newly synthesized chromophores **7**–**9**. We have also investigated the photophysical behaviour (absorption and emission) of the cation radical of these dyads.

Results and Discussion

Synthesis

The designs of the triphenylamine precursors were rationalized in order to realize nucleophilic aromatic mono- or disubstitution of chloro-*s*-tetrazines. Knowing that 3,6-dichlorotetrazine **3** can undergo mono- or disubstitution with phenol compounds, we decided to synthesize (diarylamino)phenols. Triphenylamines are known to form stable cation radicals and to polymerize through the *para* position. For future applications, it was thus necessary to prepare triphenylamine compounds that bear blocking groups, such as bromo or methyl groups, in the *para* positions. Compounds **1a**, **1b** and **1c** were targeted (Figure 3).

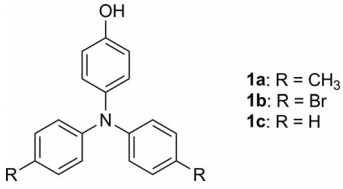

Figure 3. Design of (diarylamino)phenols.

Precursors **6a**, **6b** and **6c** were successfully prepared by Hartwig–Buchwald coupling[8] on anisidine with an excess of the corresponding bromo derivatives **2a**, **2b** or **2c** (Scheme 1). It should be noted that in the case of **6a**, the triphenylamine core was synthesized in good yield in one step, whereas with the bromo and hydrogen substituents, the preparation of the intermediate diphenylamines **5b** and **5c** were required followed by a second coupling step to obtain **6b** and **6c**, respectively, in reasonable yields. The targeted nucleophiles **1a**, **1b** and **1c** were obtained in excellent yield by using the standard deprotection of methoxyphenyl group with BBr_3[9] (Scheme 2).

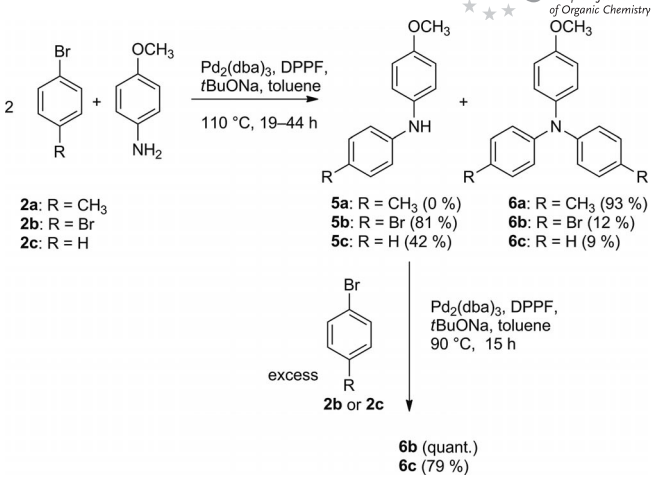

Scheme 1. Synthetic route to **6a**–**6c**.

The bichromophoric derivatives were synthesized by an S_NAr reaction with tetrazines **3** or **4**. Benefiting from the work of Hiskey and Chavez,[10] multigram syntheses of 3,6-dichlorotetrazine (**3**) and 1-chloro-6-methoxytetrazine (**4**) have been optimized by our group.[1a] The nucleophilic aromatic monosubstitution of **3** or **4** has been studied in the presence of 1 equiv. of collidine with a variety of nucleophiles, in particular, with alcohols[1d,11] and phenols:[1d,2,12] mono- and disubstitution of **3** can occur. Disubstitution is usually more difficult than monosubstitution, and it was necessary to strengthen the conditions by heating or by using a sealed tube. The introduction of 1 equiv. of **1a**, **1b** and **1c** to **3** was realized at room temperature to afford **7a**, **7b** and **7c**, respectively, in good yields (59–100%, Scheme 2).

The disubstitution of **3** or the monosubstitution of **4** appeared to be more difficult; as predicted, heating at 160 °C in a sealed tube for 1 week gave **9a**, **9b**, **8a**, **8b** and **8c** with varying yields (16–64%, Scheme 3). In the case of **9a**, after 1 week, **4** and **1b** were still present in the mixture as judged by TLC. Purification was first carried out by chromatography, which gave fractions of a mixture of **4** and **9a**. These were purified by the sublimation of **4** under reduced pressure, which left pure **9a** in a yield of 16%. For **9b**, the conversion of **1b** was very poor; degradation of the mixture led us to stop the reaction before total conversion of **1b** had been reached, which explains the yield of 31%.

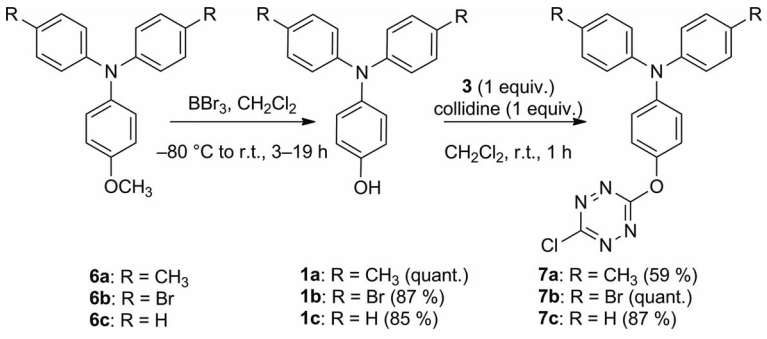

Scheme 2. Synthetic route to **7a**–**c**.

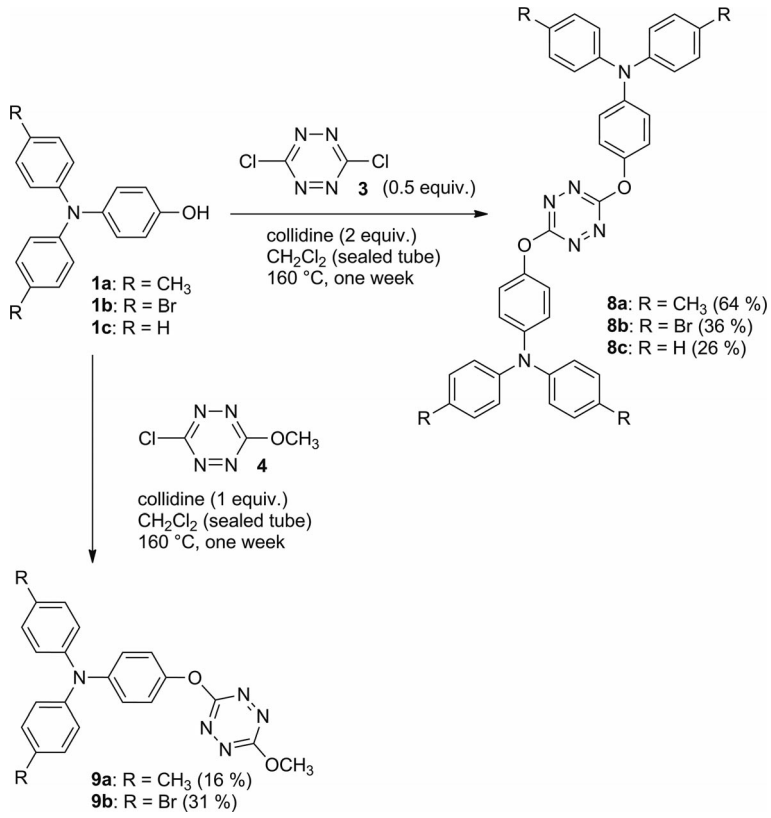

Scheme 3. Synthetic routes to **8** and **9**.

Hence, the syntheses of new bichromophoric compounds based on tetrazine and triphenylamine moieties were successfully realized in few steps by using the key S_NAr step with **3** and **4**.

Electrochemistry

The redox properties of **7**–**9** were investigated by cyclic voltammetry (CV), and the electrochemical data are summarized in Table 1. Two well-defined redox systems were identified, which correspond to the oxidation of the triphenylamine moiety into its cation radical and to the reduction of the tetrazine moiety into its anion radical. These peaks are fully reversible although the peak-to-peak separation is larger than 60 mV due to electron-transfer kinetics, which have been previously discussed for tetrazine.[11] One exception is the case of H-substituted **7c** and **8c** where polymerization occurred upon oxidation, which was expected because the *para* positions of triphenylamine were free.[13]

The data reported in Table 1 show that the standard potential of the triphenylamine moiety seems to be insensitive to the other substituent of tetrazine but depends on the nature of substituent in the *para* position. The electron-withdrawing bromine atom (**7b**, **8b** and **9b**) increases the potential of the oxidation, because it destabilizes the cation radical in comparison to the methyl group (**7a**, **8a** and **9a**). Therefore, the formation of the cation radicals of **7b**, **8b** and **9b** is more difficult and requires the application of a higher potential than triphenylamine that bears a methyl group by approximately 0.2 V. This is close to the difference between tris(4-bromophenyl)amine and tris(4-tolyl)amine.[14]

Table 1. Electrochemical data for **7**–**9**. Potentials [V] are referenced to Ag^+/Ag. The reference electrode was checked vs. ferrocene. All measurements in dichloromethane + Bu_4NPF_6 on C.

	$E°_{Tz}$[a]	$E°_{TPA}$[b]
7a	–0.83	0.48
8a	–1.12	0.48
9a	–1.08	0.51
7b	–0.77	0.72
8b	–0.94	0.75
9b	–1.01	0.70
7c	–0.98	0.67 [c]
8c	–1.05	0.55 [c]

[a] Tz = tetrazine. [b] TPA = triphenylamine. [c] Estimated value for the first cycle.

The standard potential of tetrazine depends on the atom that it is directly linked to. A chlorine atom as the electron-withdrawing group (**7a** and **7b**) stabilizes the anion radical better than an oxygen linker (**8a**, **8b**, **9a** and **9b**), which makes the reduction easier as in the parent chloro(methoxy)- and dimethoxytetrazine derivatives.[1d] The tetrazine potential is insensitive to the number of triphenylamine moieties linked to the tetrazine. This means that there is no real conjugation between triphenylamine and tetrazine in the different bichromophoric compounds. In the case of **9a** and **8b**, the results are in agreement with the expected 1:1 and 2:1 exchange ratios, respectively (Figure 4).

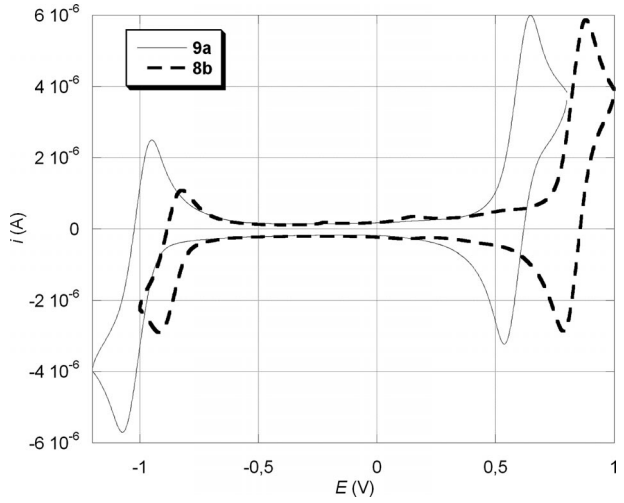

Figure 4. CVs of **8b** and **9a** in dichloromethane + 0.1 M Bu_4NPF_6 on C. Potentials referenced to Ag^+/Ag. Scan rate: 100 mV s^{-1}.

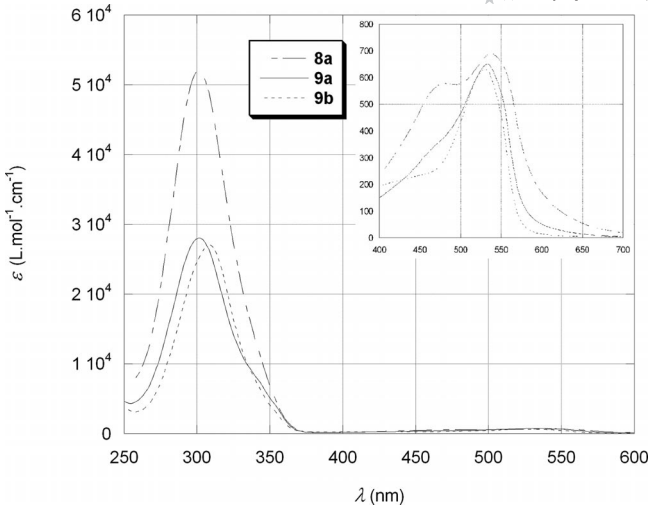

Figure 5. Molar absorption coefficients of **8a**, **9a** and **9b** in dichloromethane. Inset: molar absorption coefficients of **8a**, **9a** and **9b** in the 400–700 nm region.

In conclusion, the two redox moieties are electroactive and behave independently in the dyads.

Photophysical Properties

The absorption spectra of some of these newly synthesized compounds are displayed in Figure 5, and the absorption data are collected in Table 2. The absorption properties of the dyads are similar to the sum of the disconnected parts. These bichromophores display two or three bands depending on the substitution of the tetrazine moiety. For all of the compounds, there is an intense band in the UV region in agreement with π–π* transitions located on the tetrazine and triphenylamine units. The corresponding molar absorption coefficient is ca. 30000 L mol^{-1} cm^{-1} for compounds with one triphenylamine unit, 25000 L mol^{-1} cm^{-1} for **6a** and ca. 5000 L mol^{-1} cm^{-1} for the tetrazine derivatives.[1e] For **8a** and **8b**, the molar absorption coefficient is nearly twice that of **7a** and **7b**, respectively, because of the presence of two triphenylamine units. The second band is located at ca. 530 nm and displays a weak molar absorption coefficient (ca. 600 L mol^{-1} cm^{-1}) because of a forbidden n–π* transition centred on the tetrazine unit. This transition is also very weakly sensitive to the substituent effects on the triphenylamine moiety.[1a,1d] The third band appears only for the homodisubstituted tetrazines (**8a** and **8b**) and is located at ca. 460 nm. Its molar absorption coefficient is also very low (ca. 600 L mol^{-1} cm^{-1}), because there is a very weak orbital overlap in this transition (see theoretical calculations section).

By comparing the substitution with a bromine atom or a methyl group, one can observe that there is no influence on the n–π* transition, but there is a weak bathochromic shift (ca. 8 nm) for the π–π* transitions in the UV region, and a hypsochromic shift can be observed for the third band. An explanation for this shift is given in the theoretical calculations section.

Table 2. Photophysical properties for **6**–**9** in dichloromethane: absorption wavelength [λ_{max}, nm], molar absorption coefficient [ε, L mol^{-1} cm^{-1}], emission wavelength [λ_{em}, nm], fluorescence quantum yield [ϕ_F].

	λ_{max}	ε	λ_{max}	ε	λ_{max}	ε	λ_{em}	ϕ_F
6a	301	25000	–	–	–	–	382	0.04[a]
6b	304	26000	–	–	–	–	389	0.001[a]
7a	299	28000	–	–	523	580	550	0.0006[b]
8a	301	52000	476	686	536	690	–	–
9a	301	28000	–	–	533	650	551	0.0003[b]
7b	309	32000	–	–	524	540	559	0.001[b]
8b	309	67000	455	450	536	600	–	–
9b	308	27000	–	–	532	630	n.d.[c]	n.d.[c]

[a] Fluorescence quantum yield measured with coumarin 153 in ethanol as a standard (ϕ_F = 0.53).[15] [b] Fluorescence quantum yield measured with quinine sulfate in H_2SO_4 (0.5 N) as a standard (ϕ_F = 0.546).[16] [c] Not determined.

Even if the triphenylamine and tetrazine units are fluorescent when they are disconnected, our bichromophoric compounds are not fluorescent in their neutral state as expected. In fact, fluorescence quenching occurs because of the proximity of the two moieties through a photoinduced electron transfer from the triphenylamine unit to the tetrazine unit, as it was reported for a solution of disconnected parts.[1d] For all of the bichromophoric compounds, the fluorescence quantum yields are lower than 10^{-3}. An estimation for **7a**, **9a** and **7b** is provided in Table 2. For example, the fluorescence quantum yield of **7a** is 0.0006 even if it is 0.04 for **6a**, and 0.38[1a] for **4**.

Fluorescent Switching

In their neutral state, there is no fluorescence of the bichromophoric compounds. The fluorescence of both triphenylamine[17] and tetrazine[1] are cancelled out by an electron transfer from triphenylamine to tetrazine. When triphenylamine is oxidized, the electron transfer should not

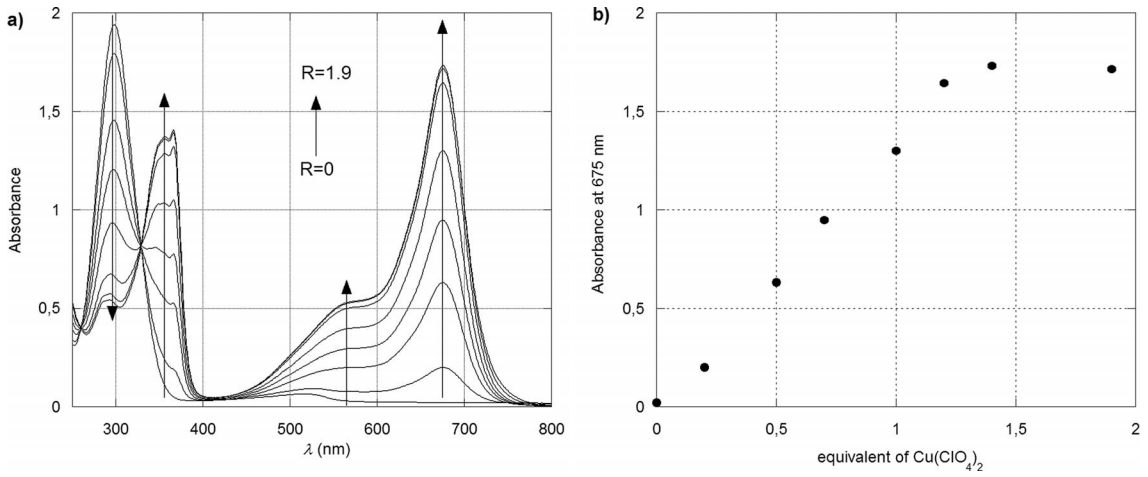

Figure 6. (a) Absorption spectra recorded upon oxidation of **7a** by $Cu(ClO_4)_2$ in CH_3CN as a function of $R = [Cu^{II}]/[\mathbf{7a}]$. Bichromophore concentration: 7×10^{-5} mol L^{-1}. (b) Correlation of the absorbance at 675 nm with the amount of $Cu(ClO_4)_2$.

occur, and thus the fluorescence of tetrazine should be restored (Figure 1). To confirm this assumption, triphenylamine was chemically oxidized to its cation radical.

The generation of the triphenylaminium cation can be achieved either by electrochemical or chemical oxidation. Although electrochemical anodic oxidation provides clean oxidation, it is difficult to complete and to study the transient species. Therefore, a one-electron chemical oxidation was chosen, and $Cu(ClO_4)_2$ was used as a mild and clean oxidant, which has been recently reported to effectively generate arylaminium cation radicals.[18] Another advantage of using $Cu(ClO_4)_2$ is that it gives no absorption or emission in the UV/Vis region at low concentrations, and its reduction potential in acetonitrile is 0.7 V vs. Fc/Fc^+, which matches the arylamines well.[18] It was therefore possible to oxidize the bichromophoric compounds. The cation radicals of the bichromophoric compounds and **6a** were thus generated by using $Cu(ClO_4)_2$ in acetonitrile and characterized by absorption and emission spectroscopy.

Upon titration with $Cu(ClO_4)_2$, one can observe the appearance of isosbestic points in the UV/Vis absorption measurements: one at ca. 260 nm and another at 329, 328, 326 and 333 nm, respectively, for **7a**, **8a**, **9a** and **7b**, which is in agreement with an equilibrium between the dyad and the oxidized triphenylamine chromophore. Two bands gradually appear at ca. 350 and 680 nm and a new shoulder emerges at 575 nm, whereas the absorption band centred at 300 nm (π–π* transition located on triphenylamine) decreases (Figure 6a; see Figures S2a, S3a and S4a, Supporting Information). When oxidation is complete, one can see the π–π* transition located on tetrazine at the same wavelength. The new absorption bands are attributed to the formation of the cation radical centred on the triphenylamine core by comparison with the absorption spectrum of the radical cation of **6a** (Figure S5a).

The correlation of the absorbance for the lower energy band with the amount of $Cu(ClO_4)_2$ revealed that all of the compound is oxidized when 1.25 equiv. of $Cu(ClO_4)_2$ was added for **7a** (Figure 6b), 2 equiv. for **8a**, 1.7 equiv. for **9a** and at least 2.5 equiv. for **7b** for a concentration of ca. 7×10^{-5} mol L^{-1} (Figures S2b, S3b and S4b). This is in line with the one-electron reduction of $Cu(ClO_4)_2$ and the number of triphenylamine units to oxidize (the two units are oxidized at the same potential in the homodisubstituted chromophores). By comparing the number of equivalents for **7a** and **7b**, one can see that the ratio is close to two, because it is more difficult to oxidize **7b** than **7a**, which is in agreement with a potential difference of around zero for **7b** and 0.22 V for **7a**.

The fluorescence spectra were recorded upon oxidation in the same $[Cu^{II}]/[\text{dyad}]$ ratios as those used for the spectrophotometric titrations but lower concentrations (ca. 7×10^{-6} mol L^{-1}) in order to avoid reabsorption artefacts.

Figure 7 displays the spectral evolution upon oxidation by excitation at the isosbestic point (329 nm) for **7a**. One can observe a linear enhancement of fluorescence upon oxidation by $Cu(ClO_4)_2$, which is in accord with the formation

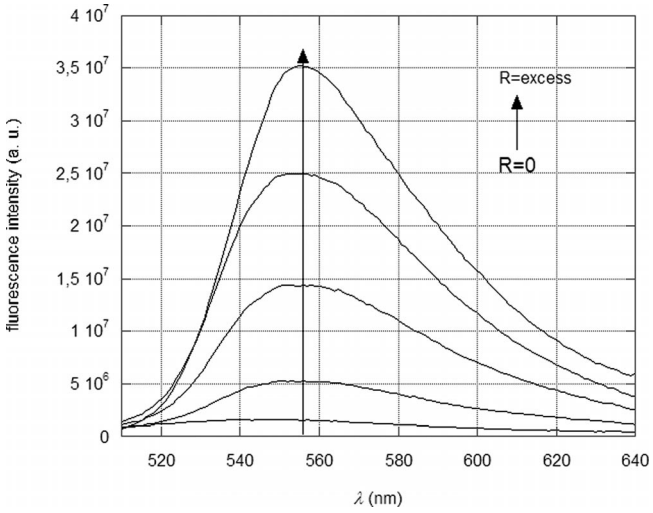

Figure 7. Emission spectra recorded upon oxidation of **7a** by $Cu(ClO_4)_2$ in CH_3CN as a function of $R = [Cu^{II}]/[\mathbf{7a}]$. Bichromophore concentration: 7.4×10^{-6} mol L^{-1}. λ_{exc} = 329 nm.

of the cation radical. In order to prove the origin of this band, the cation radical of **6a** was studied by emission spectroscopy. No fluorescence in this region was observed for this cation radical (Figure S5b). The appearance of an emission band at ca. 560 nm is typical of the tetrazine moiety.[1a]

By oxidation of the triphenylamine unit, the photoinduced electron transfer from triphenylamine to tetrazine was cancelled out, and fluorescence of the tetrazine was restored as expected. The fluorescence is multiplied by 17, 7 and 4 for **7a**, **9a** and **7b**, respectively, but the fluorescence quantum yields of the cation radical remain low (Table 3). These values are unfortunately still far from the value for **4** (0.38).[1a] This can be explained by a possible energy transfer in the cation radical because of an overlap of its absorbance and its emission (Figures 6 and 7).

Table 3. Fluorescence quantum yields for **7a**, **9a** and **7b** with R = [Cu^{II}]/[dyad].[a]

	R = 0.5	R = 1	R = 1.5	R = excess
7a	0.0018	0.0045	0.0076	0.01
9a	–	–	–	0.0065
7b	–	–	–	0.0013

[a] Measurements in acetonitrile. Fluorescence quantum yield measured with coumarin 153 in ethanol as a standard (Φ_F = 0.53).[15]

Thus, new bichromophoric compounds based on triphenylamine and tetrazine were designed and synthesized that have two states: a neutral state, in which the bichromophore is not fluorescent, whereas the cation radical is fluorescent. A fluorescent switch by oxidation was obtained.

Theoretical Calculations

Quantum chemical calculations were carried out on **7a**, **8a**, **9a** and **7b**. Geometry optimizations were first performed at the B3LYP level of theory and with the 3-21g basis set. Time-dependant (TD)DFT calculations at the PBE0 level of theory with the 6-31+g(d) basis set were subsequently performed.

In each case, the two aromatic cycles (tetrazine and phenyl rings) bound by the oxygen atom are in the same plane, whereas the two other phenyl rings of triphenylamine make a small angle with this plane (Figure 8).

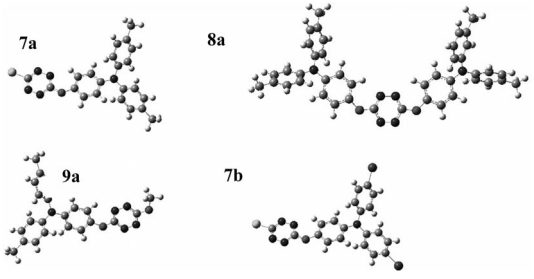

Figure 8. Calculated geometries of **7a**, **8a**, **9a** and **7b**.

The molecular orbitals are localized on each chromophore. The highest occupied molecular orbital (HOMO) is always a π orbital centred on the triphenylamine, which reflects its electron-donating ability. The nonbonding orbital of the tetrazine is found at lower energy. Conversely, the lowest unoccupied molecular orbital (LUMO) is a π* orbital centred on the tetrazine ring.

All compounds show one absorption band at ca. 300 nm (for H- or CH_3-substituted triphenylamine) or 310 nm (for Br-substituted triphenylamine). This absorption band is due to two types of transition: one from the HOMO to the π* orbital (L+1) centred on the tetrazine and the phenyl ring and the second from the HOMO to the π* orbital (L+3) centred on the diphenylamine (Figure 9). The important overlap between the orbitals of the latter transition explains the intense absorption. A weak transition is found at ca. 524 nm [for alkoxy(chloro)tetrazines] or 535 nm (for tetrazines linked to two oxygen atoms), which is localized on the tetrazine ring (n–π*) and the difference of symmetry of the H-4 orbitals and the LUMO explains the weak oscillator strength found experimentally (Table 4). Calculations show also a weak bathochromic shift when a chlorine atom replaces the oxygen atom. Indeed, chlorine stabilizes full n orbitals better than empty π* orbitals. Finally, for these bands, calculations fit well with experimental data both for wavelengths and molar absorbance coefficients (Table 4).

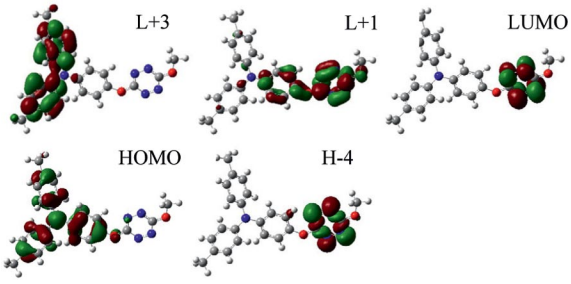

Figure 9. Representation of the main molecular orbitals involved in the electronic transitions of **9a**.

Table 4. Experimental and calculated absorption wavelengths [λ, nm] and molar absorption coefficients [ε, L mol^{-1} cm^{-1}] for **7a**, **8a**, **9a** and **7b** in vacuo [TD-DFT, PBE0, 6-31+ g(d)].

	λ_{1exp}	λ_{1calc}	ε_{1exp}	ε_{1calc}	λ_{2exp}	λ_{2calc}	ε_{2exp}	ε_{2calc}
7a	299	307	28000	31000	523	533	580	400
7b	309	314	32000	30000	524	533	540	400
8a	301	350	52000	65000	536	540	690	500
9a	301	336	28000	38000	533	538	650	300

Symmetrical **8a** and **8b** also exhibit a weak band at 455 and 475 nm, respectively, which does not exist for the unsymmetrical compounds. This absorption band is not seen by calculations performed in vacuo for **8a**. Therefore, calculations in dichloromethane have been performed by using the integral-equation formalism polarizable continuum model. Thus, **8a** displays a band at 422 nm due to a transition from a π orbital centred on the triphenylamine (H-2, see Figure S8) to the LUMO (π* orbital centred on the tetrazine). This is an intramolecular charge-transfer band.

Experimentally, the cation radical of **9a** shows two important bands at 362 and 683 nm, a shoulder at 580 nm and a weak band at 292 nm. Calculations have been performed

on the cation radical of **9a**, and Figure 10 shows the charge localization on this cation radical. One can observe that the unpaired electron is localized on the triphenylamine core as expected. The band at 730 nm is due to a transition from the π orbital centred on the tetrazine (S-2) to the SOMO (Figure 11). The shoulder has been modelled by two transitions: one from a π orbital centred on the diphenylamine part (S-3) to the SOMO at 620 nm and the second from a π orbital centred on the phenyl (S-6) to SOMO at 571 nm. The n–π* transition on the tetrazine ring is found at 538 nm. The band at 362 nm is also due to two transitions: one from the SOMO to a π* orbital centred on the diphenylamine unit (S+4) at 340 nm and the second from the HOMO to a π* orbital centred on the phenyl ring (S+2) at 338 nm.

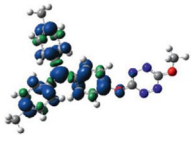

Figure 10. Spin density on the cation radical of **9a**.

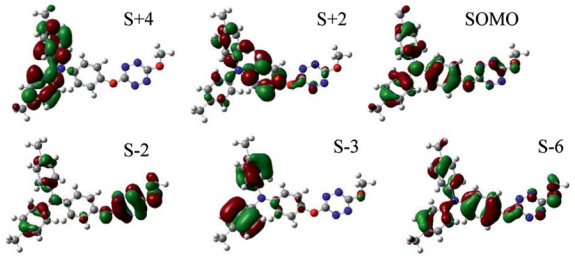

Figure 11. Representation of the main molecular orbitals involved in the electronic transitions of the cation radical of **9a**.

Conclusions

Dyads based on tetrazine–triphenylamine units have been synthesized, and their photophysical and electrochemical properties have been investigated. The generation of triphenylaminium cations was achieved by chemical oxidation and their photophysical properties have also been investigated. It appears that for unsymmetrical dyads (**7** and **9**), the absorption properties are similar to the disconnected parts, and for symmetrical dyads (**8**), another transition between a π orbital centred on triphenylamine and a π* orbital centred on tetrazine was observed, which is supported by theoretical calculations. As expected, the bichromophores exhibit very low fluorescence quantum yields in their neutral state because of a photoinduced electron transfer from the triphenylamine part to the tetrazine part. By the formation of cation radicals, the emission of tetrazine was restored, although fluorescence quantum yields remain low because of a possible energy transfer. In order to avoid this transfer and to enhance the fluorescence quantum yield, the design of new bichromophores with a bathochromic shift of the cation radical absorption is in progress.

A fluorescent switch by oxidation was designed, which features a neutral state without fluorescence and a stable cation radical state with restored fluorescence. We are currently trying to achieve a third state with these dyads with restored fluorescence of the triphenylamine moiety by reducing the tetrazine ring. Fluorescence modulation by electrochemistry[1a,3d,19] could be also performed by coupling to epifluorescence microscopy, which is currently under development in our laboratory.

Experimental Section

Spectroscopic Measurements: UV/Vis absorption spectra were recorded with a Uvikon 942 spectrophotometer in 1 cm optical length quartz cuvettes. Corrected emission spectra were obtained with a Jobin–Yvon Horiba Spex FluoroMax-3 spectrofluorometer. Dichloromethane and acetonitrile (Aldrich, spectrometric grade or SDS, spectrometric grade) were employed as solvents for absorption and fluorescence measurements. The fluorescence quantum yields were determined by using coumarin 153 in ethanol as a standard (Φ_F = 0.53)[13] or quinine sulfate in H_2SO_4 (0.5 N) as a standard (Φ_F = 0.546).[14] The estimated experimental error is less than 10%. For the emission measurements, a right-angle configuration was used, the absorbance at the excitation wavelength was kept below 0.1 and the concentration below 8×10^{-6} mol L^{-1} for the unsymmetrical compounds in order to avoid reabsorption artefacts.

Electrochemistry: Solvents (SDS, HPLC grade) and electrolyte salts (Bu_4NPF_6 from Fluka, puriss.) were used without further purification. CV was performed in a three-electrode cell with a potentiostat (CH Instruments 600) driven by a PC. A carbon electrode (1 mm diameter) was used as the working electrode, and platinum wire and Ag^+ (0.01 M in acetonitrile)/Ag were used as the counter and reference electrodes, respectively. All the investigated solutions were deaerated by bubbling with argon for at least 2 min before performing the electrochemical measurements.

Quantum Chemical Calculations: Calculations were performed with the Gaussian 03 software[20] at the MESO calculation centre of the ENS Cachan (Nec TX7 with 32 processors of type Itanium 2).

Synthesis: Reagents were commercially available from Aldrich and used without further purification. Column chromatography was performed with SDS 0.040–0.063 mm silica gel. All compounds were characterized by the usual analytical methods: ^{1}H and ^{13}C NMR spectra were recorded with a JEOL ECS (400 MHz) spectrometer. All chemical shifts are referenced to the solvent peak. Melting points were measured with a Kofler melting point apparatus. IR spectra were recorded with a Nicolet Avatar 330 FTIR spectrometer. Mass spectra were recorded with a Bruker MicrOTOF – QII instrument in direct introduction ASAP in APCI mode.

***N*,*N*-Ditolyl-4-anisidine (6a):** To a solution of tris(dibenzylideneacetone)dipalladium(0) [$Pd_2(dba)_3$, 120 mg, 0.131 mmol) and 1,1′-bis(diphenylphosphanyl)ferrocene (DPPF, 140 mg, 0.258 mmol) in dry toluene (35 mL) under argon was added 4-bromotoluene (4 mL, 32.5 mmol) at room temperature. The resulting mixture was stirred for 10 min. Sodium *tert*-butoxide (2.070 g, 21.54 mmol) and 4-anisidine (0.99 g, 8.04 mmol) were added. The resulting mixture was stirred at 110 °C for 19 h, cooled to room temperature and concentrated under reduced pressure. The crude product was purified by silica gel column chromatography [petroleum ether/CH_2Cl_2

(8:2) to petroleum ether/CH_2Cl_2 (5:5)] to give **6a** (2.048 g, 93%) as a grey solid. M.p. 70 °C. ^{1}H NMR (400 MHz, $CDCl_3$): δ = 7.08–7.05 (m, 4 H), 6.97 (d, J = 8.2 Hz, 2 H), 6.84 (d, J = 8.7 Hz, 2 H), 3.82 (s, 3 H), 2.33 (s, 6 H) ppm. ^{13}C NMR (100 MHz, $CDCl_3$): δ = 155.7, 146.0, 141.4, 131.3, 129.8, 126.5, 123.2, 114.7, 55.5, 20.8 ppm. IR: $\tilde{\nu}$ = 3024–2830, 1606, 1499, 1273, 812 cm^{-1}.

***N*-(4-Bromophenyl)-4-anisidine (5b):** To a solution of $Pd_2(dba)_3$ (242 mg, 0.264 mmol) and DPPF (289 mg, 0.529 mmol) in dry toluene (70 mL) under argon was added 1,4-dibromobenzene (15.31 g, 64.90 mmol) at room temperature. The resulting mixture was stirred for 10 min. Sodium *tert*-butoxide (4.22 g, 43.90 mmol) and 4-anisidine (2.03 g, 16.5 mmol) were added, and the mixture was stirred at 110 °C for 17 h. The reaction mixture was cooled to room temperature, and water (100 mL) was added. The aqueous layer was extracted with CH_2Cl_2 (3 × 30 mL). The organic layer was dried with anhydrous sodium sulfate, filtered and concentrated under reduced pressure. The crude product was purified by silica gel column chromatography [petroleum ether/CH_2Cl_2 (8:2) to CH_2Cl_2] to give **5b** (3.681 g, 81%) as a grey solid. M.p. 84 °C. ^{1}H NMR (400 MHz, $CDCl_3$): δ = 7.29 (d, J = 8.7 Hz, 2 H), 7.06 (d, J = 8.7 Hz, 2 H), 6.89 (d, J = 8.7 Hz, 2 H), 6.76 (d, J = 8.7 Hz, 2 H), 5.52 (s, 1 H), 3.82 (s, 3 H) ppm. ^{13}C NMR (100 MHz, $CDCl_3$): δ = 155.7, 144.5, 135.1, 132.1, 122.8, 117.0, 114.8, 111.0, 55.6 ppm. IR: $\tilde{\nu}$ = 3419, 3050–2850, 1594, 1508, 1491, 1243, 1030, 813 cm^{-1}.

***N*-Phenyl-4-anisidine (5c):** To a solution of $Pd_2(dba)_3$ (137 mg, 0.150 mmol) and DPPF (130 mg, 0.238 mmol) in dry toluene (40 mL) under argon was added 4-bromobenzene (2.5 mL, 23.74 mmol) at room temperature. The resulting mixture was stirred for 10 min. Sodium *tert*-butoxide (2.564 g, 26.70 mmol) and 4-anisidine (1.233 g, 10.01 mmol) were added, and the mixture was stirred at 90 °C for 22 h. After this time, the starting materials had disappeared as judged by TLC. The reaction mixture was cooled to room temperature, and water was added. It was extracted with diethyl ether, dried with anhydrous sodium sulfate, filtered and concentrated under reduced pressure. The crude product was purified by silica gel column chromatography [petroleum ether/CH_2Cl_2 (1:1) to CH_2Cl_2] to give **5c** (1.169 g, 42%) as a grey solid. M.p. 102 °C. ^{1}H NMR (400 MHz, $CDCl_3$): δ = 7.25–7.20 (m, 2 H), 7.10–7.06 (m, 2 H), 6.93–6.82 (m, 5 H), 5.55 (s, 1 H), 3.81 (s, 3 H) ppm. ^{13}C NMR (100 MHz, $CDCl_3$): δ = 155.2, 145.2, 135.8, 129.3, 122.1, 119.6, 115.7, 114.7, 55.6 ppm. IR: $\tilde{\nu}$ = 3386, 3008–2836, 1595, 1500, 1489, 1249, 1032, 749, 694 cm^{-1}.

***N*,*N*-Bis(4-bromophenyl)-4-anisidine (6b):** To a solution of $Pd_2(dba)_3$ (282 mg, 0.308 mmol) and DPPF (230 mg, 0.421 mmol) in dry toluene (10 mL) under argon was added 1,4-dibromobenzene (5.17 mg, 21.92 mmol) at room temperature. The resulting mixture was stirred for 10 min. Sodium *tert*-butoxide (1.53 g, 15.92 mmol) and **5b** (1.12 g, 5.25 mmol) were added, and the mixture was stirred at 110 °C for 15 h. After this time, the starting materials had disappeared as judged by TLC. The reaction mixture was cooled to room temperature and concentrated under reduced pressure. The crude product was purified by silica gel column chromatography [petroleum ether/CH_2Cl_2 (8:2) to petroleum ether/CH_2Cl_2 (1:3)] to give **6b** (1.740 g, quantitative yield) as a white solid. M.p. 75 °C. ^{1}H NMR (400 MHz, $CDCl_3$): δ = 7.32 (d, J = 9.2 Hz, 4 H), 7.07 (d, J = 9.2 Hz, 2 H), 6.93 (d, J = 8.7 Hz, 4 H), 6.88 (d, J = 8.7 Hz, 2 H), 3.82 (s, 3 H) ppm. ^{13}C NMR (100 MHz, $CDCl_3$): δ = 156.7, 146.8, 139.7, 132.2, 127.4, 124.3, 115.1, 114.6, 55.5 ppm. IR: $\tilde{\nu}$ = 3050–2830, 1578, 1504, 1482, 1237, 813 cm^{-1}.

***N*,*N*-Diphenyl-4-anisidine (6c):** To a solution of $Pd_2(dba)_3$ (253 mg, 0.276 mmol) and DPPF (202 mg, 0.370 mmol) in dry toluene (40 mL) under argon was added 4-bromobenzene (1.7 mL, 16.56 mmol) at room temperature. The resulting mixture was stirred for 10 min. Sodium *tert*-butoxide (1.379 g, 14.35 mmol) and **5c** (1.100 g, 5.52 mmol) were added, and the mixture was stirred at 90 °C for 20 h. After this time, the starting materials had disappeared as judged by TLC. The reaction mixture was cooled to room temperature, and water was added. It was extracted with CH_2Cl_2, dried with anhydrous sodium sulfate, filtered and concentrated under vacuum. The crude product was purified by silica gel column chromatography [petroleum ether to petroleum ether/CH_2Cl_2 (1:1)] to give **6c** (1.069 g, 79%) as a white solid. M.p. 102 °C. ^{1}H NMR (400 MHz, $CDCl_3$): δ = 7.19 (dd, J = 8.2, 7.3 Hz, 4 H), 7.08 (m, 6 H), 6.97 (t, J = 7.3 Hz, 2 H), 6.87 (d, J = 9.2 Hz, 2 H), 3.83 (s, 3 H) ppm. ^{13}C NMR (100 MHz, $CDCl_3$): δ = 156.2, 148.3, 140.9, 129.1, 127.4, 123.0, 121.9, 114.9, 55.6 ppm. IR: $\tilde{\nu}$ = 3003–2835, 1595, 1584, 1488, 1237, 728, 692 cm^{-1}.

Procedure for the Deprotection of the Phenols: In a three-necked round-bottomed flask was placed the protected phenol compound (2.23 mmol) in anhydrous CH_2Cl_2 (30 mL). A solution of 1 M boron tribromide (3 mL, 3.00 mmol) was added dropwise at –78 °C, and the mixture was stirred at room temperature for 3 h. The mixture was poured onto ice and extracted with CH_2Cl_2 (3 × 30 mL). The organic layers were dried with anhydrous sodium sulfate, filtered and concentrated under reduced pressure. The crude product was purified by silica gel column chromatography.

4-(Ditolylamino)phenol (1a): The crude product was purified by silica gel column chromatography [petroleum ether/ethyl acetate (4:1)] to give **1a** as a white solid (quantitative yield). M.p. 68 °C. ^{1}H NMR (400 MHz, CD_3OD): δ = 7.00 (d, J = 7.8 Hz, 4 H), 6.88 (d, J = 8.7 Hz, 2 H), 6.84 (d, J = 8.2 Hz, 4 H), 6.73 (d, J = 8.7 Hz, 2 H), 2.27 (s, 6 H) ppm. ^{13}C NMR (100 MHz, CD_3OD): δ = 154.7, 147.5, 141.5, 132.1, 130.5, 128.0, 123.8, 117.0, 20.7 ppm. IR: $\tilde{\nu}$ = 3250, 3027, 1605, 1502, 1276, 1216, 813 cm^{-1}. UV/Vis (CH_2Cl_2): λ_{max} (ε, L cm^{-1} mol^{-1}) = 300 (21400); Φ_F = 0.013 in CH_2Cl_2.

4-[Bis(4-bromophenyl)amino]phenol (1b): The crude product was purified by silica gel column chromatography [petroleum ether/ethyl acetate (4:1)] to give **1b** (714 mg, 87%) as a white solid. ^{1}H NMR (400 MHz, $CDCl_3$): δ = 7.29 (d, J = 8.7 Hz, 4 H), 6.98 (d, J = 8.7 Hz, 2 H), 6.90 (d, J = 8.7 Hz, 4 H), 6.84 (d, J = 8.7 Hz, 2 H) ppm. ^{13}C NMR (100 MHz, $CDCl_3$): δ = 153.4, 146.8, 139.3, 132.1, 127.7, 124.2, 116.6, 114.4 ppm.

4-(Diphenylamino)phenol (1c): The crude product was purified by silica gel column chromatography [petroleum ether/CH_2Cl_2 (1:1) to CH_2Cl_2/ethanol (85:15)] to give **1c** (777 mg, 85%) as a grey solid. M.p. 121 °C. ^{1}H NMR (400 MHz, $CDCl_3$): δ = 7.26–7.18 (m, 4 H), 7.11–6.89 (m, 8 H), 6.85–6.7 (m, 2 H), 5.07 (S, 1 H) ppm. ^{13}C NMR (100 MHz, $CDCl_3$): δ = 152.0, 148.2, 141.0, 129.2, 127.6, 123.0, 122.0, 116.4 ppm. IR: $\tilde{\nu}$ = 3300, 3050–2830, 1584, 1506, 1488, 1281, 1229, 752, 694 cm^{-1}.

Procedure for the S_NAr Reaction with 3,6-Dichlorotetrazine: To a solution of the phenol compound (1.14 mmol) in anhydrous CH_2Cl_2 (25 mL) were added 3,6-dichlorotetrazine (1.14 mmol) and 2,4,6-collidine (1.14 mmol). The mixture was stirred at room temperature for 1 h and concentrated under reduced pressure. The crude product was purified by silica gel column chromatography.

3-Chloro-6-[4-(ditolylamino)phenoxy]-1,2,4,5-tetrazine (7a): The crude product was purified by silica gel column chromatography [petroleum ether/CH_2Cl_2 (1:1)] to give **7a** (270 mg, 59%) as a purple solid. M.p. 170 °C. ^{1}H NMR (400 MHz, $CDCl_3$): δ = 7.10–7.07 (m, 8 H), 7.02 (d, J = 8.7 Hz, 4 H), 2.32 (s, 6 H) ppm. ^{13}C NMR (100 MHz, $CDCl_3$): δ = 167.9, 165.2, 147.2, 145.6, 145.1, 133.2, 130.2, 125.0, 123.1, 121.3, 21.0 ppm. IR: $\tilde{\nu}$ = 3050–2850, 1604,

1497, 1432, 1354, 1274, 1154, 819 cm^{-1}. HRMS: calcd. for $C_{22}H_{18}N_5O^{35}Cl$ $[M]^+$ 403.11944; found 403.1194.

3-{4-[Bis(4-bromophenyl)amino]phenoxy}-6-chloro-1,2,4,5-tetrazine (7b): The crude product was purified by silica gel column chromatography [petroleum ether/CH_2Cl_2 (7:3) to petroleum ether/CH_2Cl_2 (4:6)] to give **7b** as a red solid (quantitative yield). M.p. 154 °C. ^1H NMR (400 MHz, $CDCl_3$): δ = 7.38 (d, J = 8.7 Hz, 4 H), 7.15–7.14 (m, 4 H), 6.97 (d, J = 8.7 Hz, 4 H) ppm. ^{13}C NMR (100 MHz, $CDCl_3$): δ = 167.7, 165.4, 147.1, 146.2, 145.8, 132.7, 125.9, 125.2, 121.9, 116.3 ppm. IR: $\tilde{\nu}$ = 1578, 1502, 1484, 1358, 1270, 823 cm^{-1}. HRMS: calcd. for $C_{20}H_{12}N_5O^{35}Cl^{79}Br_2$ $[M]^+$ 530.90916; found 530.9091.

3-Chloro-6-[4-(diphenylamino)phenoxy]-1,2,4,5-tetrazine (7c): The crude product was purified by silica gel column chromatography [petroleum ether to petroleum ether/CH_2Cl_2 (2:8)] to give **7c** (113 mg, 87%) as a red solid. M.p. 102 °C. ^1H NMR (400 MHz, $CDCl_3$): δ = 7.28 (dd, J = 8.2, 7.3 Hz, 4 H), 7.16–7.11 (m, 8 H), 7.08–7.03 (m, 2 H) ppm. ^{13}C NMR (100 MHz, $CDCl_3$): δ = 167.9, 165.3, 147.6, 146.8, 146.4, 129.6, 124.7, 124.5, 123.5, 121.5 ppm. IR: $\tilde{\nu}$ = 3050–2830, 1591, 1502, 1492, 1358, 1278, 1200, 843, 813 cm^{-1}.

Procedure for the S_NAr Reaction with 3-Chloro-6-methoxy-1,2,4,5-tetrazine: To a solution of the phenol compound (1.17 mmol) in anhydrous CH_2Cl_2 (25 mL) were added 3-chloro-6-methoxytetrazine (1.17 mmol) and 2,4,6-collidine (1.17 mmol). The mixture was stirred at 150 °C in a sealed tube for 1 week and concentrated under reduced pressure. The crude product was purified by silica gel column chromatography.

3-[4-(Ditolylamino)phenoxy]-3-methoxy-1,2,4,5-tetrazine (9a): The crude product was purified by silica gel column chromatography [petroleum ether/CH_2Cl_2 (3:7)] to give **9a** (74 mg, 16%) as a red solid. M.p. 190 °C. ^1H NMR (400 MHz, $CDCl_3$): δ = 7.10–7.05 (m, 8 H), 7.00 (d, J = 8.2 Hz, 4 H), 4.26 (s, 3 H), 2.31 (s, 6 H) ppm. ^{13}C NMR (100 MHz, $CDCl_3$): δ = 167.3, 166.7, 146.8, 146.5, 145.2, 132.8, 130.1, 124.7, 123.6, 121.5, 57.0, 20.9 ppm. IR: $\tilde{\nu}$ = 3050–2850, 1605, 1497, 1441, 1370, 1274, 1197, 818 cm^{-1}. HRMS: calcd. for $C_{23}H_{21}N_5O_2$ $[M]^+$ 399.16898; found 399.1683.

3-{4-[Bis(4-bromophenyl)amino]phenoxy}-3-methoxy-1,2,4,5-tetrazine (9b): The crude product was purified by silica gel column chromatography [petroleum ether/CH_2Cl_2 (7:3) to petroleum ether/CH_2Cl_2 (1:1)] to give **9b** as a red solid (31%). M.p. 140 °C. ^1H NMR (400 MHz, $CDCl_3$): δ = 7.35 (d, J = 8.7 Hz, 4 H), 7.17–7.11 (m, 4 H), 6.97 (d, J = 9.2 Hz, 4 H), 4.27 (s, 3 H) ppm. ^{13}C NMR (100 MHz, $CDCl_3$): δ = 167.1, 166.8, 148.2, 146.3, 145.1, 132.6, 125.7, 125.5, 122.0, 116.0, 57.1 ppm. IR: $\tilde{\nu}$ = 3050–2850, 1576, 1500, 1484, 1379, 1270, 1206, 823 cm^{-1}. HRMS: calcd. for $C_{21}H_{15}N_5O_2{}^{79}Br_2$ $[M]^+$ 526.9587; found 526.9588.

Procedure for the S_NAr Disubstitution Reaction with 3,6-Dichlorotetrazine: To a solution of the phenol compound (1.50 mmol) in anhydrous CH_2Cl_2 (8 mL) were added 3,6-dichlorotetrazine (0.75 mmol) and 2,4,6-collidine (1.50 mmol). The mixture was stirred at 160 °C in a sealed tube for 1 week and concentrated under reduced pressure. The crude product was purified by silica gel column chromatography.

3,6-Bis[4-(ditolylamino)phenoxy]-1,2,4,5-tetrazine (8a): The crude product was purified by silica gel column chromatography [petroleum ether/CH_2Cl_2 (5:5)] to give **8a** (303 mg, 64%) as a purple solid. M.p. 170 °C. ^1H NMR (400 MHz, $CDCl_3$): δ = 7.15–7.05 (m, 16 H), 7.04 (d, J = 8.2 Hz, 8 H), 2.34 (s, 12 H) ppm. ^{13}C NMR (100 MHz, $CDCl_3$): δ = 167.5, 146.6, 146.5, 145.2, 132.9, 130.1, 124.8, 123.6, 121.5, 20.9 ppm. IR: $\tilde{\nu}$ = 3000–2850, 1604, 1497, 1432, 1355, 1273, 1155, 819 cm^{-1}. HRMS: calcd. for $C_{42}H_{36}N_6O_2$ $[M]^+$ 656.28942; found 656.2892.

3,6-Bis{4-[bis(4-bromophenyl)amino]phenoxy}-1,2,4,5-tetrazine (8b): The crude product was purified by silica gel column chromatography [petroleum ether/CH_2Cl_2 (7:3) to CH_2Cl_2] to give **8b** as a pink solid (36%). M.p. 148 °C. ^1H NMR (400 MHz, $CDCl_3$): δ = 7.37 (d, J = 8.7 Hz, 8 H), 7.17–7.10 (m, 8 H), 6.96 (d, J = 8.7 Hz, 8 H) ppm. ^{13}C NMR (100 MHz, $CDCl_3$): δ = 167.5, 148.0, 146.3, 145.4, 132.7, 125.8, 125.4, 122.1, 116.2 ppm. IR: $\tilde{\nu}$ = 2988, 1579, 1501, 1483, 1398, 1267, 825 cm^{-1}. HRMS: calcd. for $C_{38}H_{24}N_6O_2{}^{79}Br_4$ $[M]^+$ 911.86887; found 911.8684.

3,6-Bis[4-(diphenylamino)phenoxy]-1,2,4,5-tetrazine (8c): The crude product was purified by silica gel column chromatography [petroleum ether/CH_2Cl_2 (1:1) to CH_2Cl_2/ethanol (95:5)] to give **8c** (174 mg, 26%) as a red powder. M.p. 236 °C. ^1H NMR (400 MHz, $CDCl_3$): δ = 7.27 (dd, J = 8.7, 7.3 Hz, 8 H), 7.14–7.09 (m, 16 H), 7.03 (t, J = 7.3 Hz, 4 H) ppm. ^{13}C NMR (100 MHz, $CDCl_3$): δ = 167.5, 147.7, 147.3, 146.3, 129.5, 124.9, 124.5, 123.3, 121.7 ppm. IR: $\tilde{\nu}$ = 3050–2830, 1587, 1502, 1488, 1385, 1276, 1198, 755, 699 cm^{-1}.

Supporting Information (see footnote on the first page of this article): CV data, photophysical data and theoretical data.

Acknowledgments

We thank the CNRS and the Ministry of French Research for funding the project. We also thank Dr C. Allain for fruitfull discussions.

[1] a) G. Clavier, P. Audebert, *Chem. Rev.* **2010**, *110*, 3299–3314; b) P. Audebert, S. Sadki, F. Miomandre, G. Clavier, *Electrochem. Commun.* **2004**, *6*, 144–147; c) P. Audebert, S. Sadki, F. Miomandre, G. Clavier, M. C. Vernieres, M. Saoud, P. Hapiot, *New J. Chem.* **2004**, *28*, 387–392; d) P. Audebert, F. Miomandre, G. Clavier, M. C. Vernières, S. Badré, R. Méallet-Renault, *Chem. Eur. J.* **2005**, *11*, 5667–5673; e) Y.-H. Gong, F. Miomandre, R. Méallet-Renault, S. Badré, L. Galmiche, J. Tang, P. Audebert, G. Clavier, *Eur. J. Org. Chem.* **2009**, *35*, 6121–6128.

[2] C. Dumas-Verdes, F. Miomandre, E. Lépicier, O. Galangau, T. T. Vu, G. Clavier, R. Méallet-Renault, P. Audebert, *Eur. J. Org. Chem.* **2010**, *13*, 2525–2535.

[3] a) Y. Kim, E. Kim, G. Clavier, P. Audebert, *Chem. Commun.* **2006**, *34*, 3612–3614; b) Y. Kim, J. Do, E. Kim, G. Clavier, L. Galmiche, P. Audebert, *J. Electroanal. Chem.* **2009**, *632*, 201–205; c) F. Miomandre, R. Méallet-Renault, J. J. Vachon, R. Pansu, P. Audebert, *Chem. Commun.* **2008**, *16*, 1913–1915; d) F. Miomandre, E. Lépicier, S. Munteanu, O. Galangau, J. F. Audibert, R. Méallet-Renault, P. Audebert, R. B. Pansu, *ACS Appl. Mater. Interfaces* **2011**, *3*, 690–696.

[4] a) A. C. Benniston, G. Copley, K. J. Elliott, R. W. Harrington, W. Clegg, *Eur. J. Org. Chem.* **2008**, *16*, 2705–2713; b) R. Zhang, Z. Wang, Y. Wu, H. Fu, J. Yao, *Org. Lett.* **2008**, *10*, 3065–3068.

[5] a) U. Resch-Genger, G. Hennrich in *Topics in Fluorescence Spectroscopy* (Eds.: C. D. Geddes, J. R. Lakowicz), Springer US, **2005**, vol. 9, pp. 189–218; b) T. Komura, G. Y. Niu, T. Yamaguchi, M. Asano, *Electrochim. Acta* **2003**, *48*, 631–639; c) R. Bergonzi, L. Fabbrizzi, M. Licchelli, C. Mangano, *Coord. Chem. Rev.* **1998**, *170*, 31–46; d) R. W. Wagner, J. S. Lindsey, J. Seth, V. Palaniappan, D. F. Bocian, *J. Am. Chem. Soc.* **1996**, *118*, 3996–3997; e) J. Otsuki, M. Tsujino, T. Iizaki, K. Araki, M. Seno, K. Takatera, T. Watanabe, *J. Am. Chem. Soc.* **1997**, *119*, 7895–7896; f) G. Hennrich, H. Sonnenschein, U. Resch-Genger, *J. Am. Chem. Soc.* **1999**, *121*, 5073–5074; g) R. Zhang, Z. Wang, Y. Wu, H. Fu, J. Yao, *Org. Lett.* **2008**, *10*, 3065–3068; h) L. Liu, G. Zhang, W. Tan, D. Zhang, D. Zhu, *Chem. Phys.*

Lett. **2008**, *465*, 230–233; i) T. Suzuki, A. Migita, H. Higuchi, H. Kawai, K. Fujiwara, T. Tsuji, *Tetrahedron Lett.* **2003**, *44*, 6837–6840.

[6] a) Y. Shirota, H. Kageyama, *Chem. Rev.* **2007**, *107*, 953; b) C. C. Chi, C. L. Chiang, S. W. Liu, H. Yueh, C. T. Chen, C. T. Chen, *J. Mater. Chem.* **2009**, *19*, 5561–5571; c) X. Liu, D. Xu, R. Lu, B. Li, C. Qian, P. Xue, X. Zhang, H. Zhou, *Chem. Eur. J.* **2011**, *17*, 1660–1669; d) Q. Li, L. Lu, C. Zhong, J. Huang, Q. Huang, J. Shi, X. Jin, T. Peng, J. Qin, Z. Li, *Chem. Eur. J.* **2009**, *15*, 9664–9668; e) B. Wang, Y. Wang, J. Hua, Y. Jiang, J. Huang, S. Qian, H. Tian, *Chem. Eur. J.* **2011**, *17*, 2647–2655.

[7] B. Lim, Y. C. Nah, J. T. Hwang, J. Ghim, D. Vak, J. M. Yun, D. Y. Kim, *J. Mater. Chem.* **2009**, *19*, 2380–2385.

[8] S. Thayumanavan, S. Barlow, S. R. Marder, *Chem. Mater.* **1997**, *9*, 3231–3235.

[9] J. G. Linkletter, G. A. Pearson, R. I. Walter, *J. Am. Chem. Soc.* **1977**, *99*, 5269–5272.

[10] a) D. E. Chavez, M. A. Hiskey, *J. Heterocycl. Chem.* **1998**, *35*, 1329; b) D. E. Chavez, M. A. Hiskey, *J. Energ. Mater.* **1999**, *17*, 357; c) M. D. Coburn, G. A. Buntain, B. W. Harris, M. A. Hiskey, K. Y. Lee, D. G. Ott, *J. Heterocycl. Chem.* **1991**, *28*, 2049.

[11] a) Y.-H. Gong, P. Audebert, J. Tang, F. Miomandre, G. Clavier, S. Badré, R. Méallet-Renault, J. Marrot, *J. Electroanal. Chem.* **2006**, *592*, 147–152; b) Y.-H. Gong, P. Audebert, G. Clavier, F. Miomandre, J. Tang, S. Badré, R. Méallet-Renault, E. Naidus, *New J. Chem.* **2008**, *32*, 1235–1242.

[12] Q. Zhou, P. Audebert, G. Clavier, R. Méallet-Renault, F. Miomandre, Z. Shaukat, T. T. Vu and J. Tang, *J. Phys. Chem. C* 2011, 115, 21899–21906.

[13] a) C. Lambert, G. Nöll, *Synth. Met.* **2003**, *139*, 57–62; b) A. Petr, C. Kvarnström, L. Dunsch, A. Ivaska, *Synth. Met.* **2000**, *108*, 245–247; c) A.-D. Bendrea, L. Vacareanu, M. Grigoras, *Polym. Int.* **2009**, *59*, 624–629; d) H.-Y. Lin, G.-S. Liou, *J. Polym. Sci. Polym. Chem. Ed.* **2009**, *47*, 285–294; e) C. Zhan, Z. Cheng, J. Zheng, W. Zhang, Y. Xi, J. Qin, *J. Appl. Polym. Sci.* **2002**, *85*, 2718–2724.

[14] K. Idzik, J. Soloducho, M. Lapkowski, S. Golba, *Electrochim. Acta* **2008**, *53*, 5665–5669.

[15] M. Grabolle, M. Spieles, V. Lesnyak, N. Gaponik, A. Eychmüller, U. Resch-Genger, *Anal. Chem.* **2009**, *81*, 6285–6294.

[16] J. N. Demas, G. A. Crosby, *J. Phys. Chem.* **1971**, *75*, 991.

[17] a) E. Ishow, A. Brosseau, G. Clavier, K. Nakatani, P. Tauc, C. l. Fiorini-Debuisschert, S. Neveu, O. Sandre, A. Léaustic, *Chem. Mater.* **2008**, *20*, 6597–6599; b) H. G. Zhang, X. T. Tao, K. S. Chen, C. X. Yuan, S. N. Yan, M. H. Jiang, *Chin. Chem. Lett.* **2011**, *22*, 647–650; c) L. Yang, F. Gao, J. Liu, X. Zhong, H. Li, S. Zhang, *J. Fluores.* **2010**, *21*, 545–554; d) B. Li, Q. Li, B. Liu, Y. Yue, M. Yu, *Dyes Pigm.* **2011**, *88*, 301–306.

[18] C.-C. Chang, H. Yueh, C.-T. Chen, *Org. Lett.* **2011**, *13*, 2702–2705.

[19] a) M. Voicescu, D. Rother, F. Bardischewsky, C. G. Friedrich, P. Hellwig, *Biochemistry* **2011**, *50*, 17–24; b) J. Daub, M. Beck, A. Knorr, H. Spreitzer, *Pure Appl. Chem.* **1996**, *68*, 1399–1404.

[20] M. J. Frisch, G. W. Trucks, H. B. Schlegel, G. E. Scuseria, M. A. Robb, J. R. Cheeseman, J. A. Montgomery Jr., T. Vreven, K. N. Kudin, J. C. Burant, J. M. Millam, S. S. Iyengar, J. Tomasi, V. Barone, B. Mennucci, M. Cossi, G. Scalmani, N. Rega, G. A. Petersson, H. Nakatsuji, M. Hada, M. Ehara, K. Toyota, R. Fukuda, J. Hasegawa, M. Ishida, T. Nakajima, Y. Honda, O. Kitao, H. Nakai, M. Klene, X. Li, J. E. Knox, H. P. Hratchian, J. B. Cross, C. Adamo, J. Jaramillo, R. Gomperts, R. E. Stratmann, O. Yazyev, A. J. Austin, R. Cammi, C. Pomelli, J. W. Ochterski, P. Y. Ayala, K. Morokuma, G. A. Voth, P. Salvador, J. J. Dannenberg, V. G. Zakrzewski, S. Dapprich, A. D. Daniels, M. C. Strain, O. Farkas, D. K. Malick, A. D. Rabuck, K. Raghavachari, J. B. Foresman, J. V. Ortiz, Q. Cui, A. G. Baboul, S. Clifford, J. Cioslowski, B. B. Stefanov, G. Liu, A. Liashenko, P. Piskorz, I. Komaromi, R. L. Martin, D. J. Fox, T. Keith, M. A. Al-Laham, C. Y. Peng, A. Nanayakkara, M. Challacombe, P. M. W. Gill, B. Johnson, W. Chen, M. W. Wong, C. Gonzalez, J. A. Pople, *Gaussian 03*, Revision C.02, Gaussian, Inc., Wallingford, CT, **2004**.

Received: October 21, 2011
Published Online: January 9, 2012

